Journal of Materials Chemistry C

Accepted Manuscript

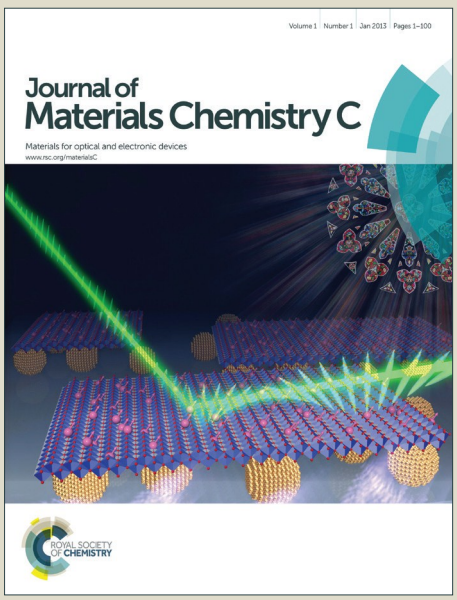

ROYAL SOCIETY OF CHEMISTRY

www.rsc.org/materialsC

Searching for fabrication route of efficient Cu_2ZnSnS_4 solar cells by post-sulfuration of co-sputtered Sn-enriched precursors

Ye Feng[1], Bing Yu[1], Guanming Cheng[1], Tszki Lau[2], Zhaohui Li[1], Ling Yin[2], Qiuming Song[1], Chunlei Yang[1,*], Xudong Xiao[2,*]

[1]*Center for Photovoltaics and Solar Energy, Shenzhen Institutes of Advanced Technology, Chinese Academy of Sciences, Shenzhen, 518055, China*

[2] *Department of Physics, The Chinese University of Hong Kong, Shatin, Hong Kong, China*

* Corresponding authors, email: cl.yang@siat.ac.cn, xdxiao@phy.cuhk.edu.hk.
Tel: +8675586392132.

Abstract

We have systematically investigated the Sn loss in Cu_2ZnSnS_4 (CZTS) thin film formation process using sputtering/sulfuration approach with highly Sn-enriched precursors. It was found that the remaining Sn content in the CZTS absorber strongly dependent on the peak sulfuration temperature, H_2S concentration in the sulfuration atmosphere, temperature ramping rate, and Zn content in the precursors. Since the Sn content could be controlled by the Sn loss during the thermal treatment process, the final composition of the CZTS thin films could be manipulated simply by tailoring the Cu/Zn ratio in the precursors. With such a route, highly efficient solar cells could be achieved from Sn-rich precursors.

Keywords: Cu_2ZnSnS_4; Sn loss; Sn-rich precursor; post-sulfuration.

1. Introduction

Kesterite $Cu_2ZnSn(S,Se)_4$ (CZTSSe) thin films have been a subject of growing scientific and technological interest because they are composed of all earth-abundant and non-toxic elements, yet are similar in crystal structure and predicted electrical properties to chalcopyrite $Cu(In,Ga)Se_2$ (CIGS) films which has already demonstrated the best photovoltaic performance among various thin film solar cells but uses rare metal elements. The past several years have witnessed dramatic improvements in the performance of kesterite devices, with IBM reporting a champion efficiency of 12.6%[1] achieved for CZTSSe by atmospheric-pressure reaction of particle-containing hydrazine solutions. For devices made of pure Cu_2ZnSnS_4 (CZTS) and $Cu_2ZnSnSe_4$ (CZTSe), the highest conversion efficiency are respectively 8.4%[2] and 9.15%[3], with both grown by co-evaporation processes. Despite these efforts, kesterites do not yet reach comparable efficiency achieved in CIGS. One of the most important reasons for the inferior performance is that CZTSSe films have a very complicated phase diagram[4] that makes both defects and secondary phases difficult to be removed.

Previous experiments have revealed that most of the best-performing devices exhibited ratios of Cu/(Zn + Sn) ~ 0.8–0.9 and Zn/Sn ~ 1.1–1.3 in the CZTSSe thin film[1-3, 5-9], and were termed copper-poor and zinc-rich accordingly. People usually judge the condition of copper-poor by the ratio of Copper to total amount of Zn and Sn, as Cu/(In+Ga) commonly used in CIGS. Actually, the respective ratios of Cu/Sn and Cu/Zn are also important because the formation process of CZTS is different from CIGS. For CZTS, quaternary compounds were formed by incorporation of Zn into the frame of ternary compounds of Cu and Sn, such as Cu_2SnS_3, because no such ternary compounds of Cu and Zn could be synthesized. The ratio of Cu/Sn should decide the properties of the intermediate compounds and also influence those of final compounds. In the post-sulfuration approach to fabricate the CZTS thin film absorbers, as $Cu_{2-x}S$ and ZnS are stable compounds under normal annealing conditions, the amounts of Cu and Zn normally remain unchanged after thermal treatment in comparison with those in the precursors. However, loss of Sn has often been observed during CZTS film synthesis[10-13] and is attributed to the evaporation of Sn related compounds at elevated temperatures. Therefore, the control of Cu/Sn is more difficult than Cu/Zn in fabricating CZTS thin film with desired compositions. Sn-poor CZTS samples with Cu/Sn >2 always possess $Cu_{2-x}S$ secondary phase which strongly deteriorates the device performance. Thus, the control of Sn loss is a prerequisite to form good Kesterite solar cells.

In this paper, we report various strategies to fabricate CZTS absorbers, starting with highly Sn-enriched precursors by co-sputtering Cu, ZnS and SnS_2 targets. We have systematically studied the dependence of Cu/Sn ratio in the prepared films on post-sulfuration parameters such as the peak annealing temperature, H_2S concentration in the annealing atmosphere, temperature ramping rate, and Zn contents. We found that the remaining Sn contents in the thin films were strongly affected by all the annealing parameters mentioned above. The ability for tailoring the elemental composition through understanding the Sn loss process during annealing would be very helpful in designing individualized annealing process for precursors with different initial compositions. With such increased flexibility, it would certainly relax the requirement for the precursor preparation, which is important to achieve commercialization success in the future.

2. Experiments

The CZTS thin films in this study were fabricated by a two-stage process which consists of precursor deposition followed by sulfuration treatment. The precursors were deposited on Mo-coated 10x10 cm^2 size soda-lime glass by simultaneously sputtering SnS_2, ZnS, and Cu targets. The co-sputtering process can presumably mix the three target materials thoroughly at nanoscale. Our precursors were different from those reported by Katagiri's group who deposited multiple stacking layers of Cu/SnS_2/ZnS which required annealing at 400°C in vacuum to promote inter-diffusion[14]. To form CZTS polycrystalline films, precursors were sulfurized in an atmosphere of N_2+H_2S with a total pressure of 300 Torr. Sulfuration conditions are varied to examine their effects in the CZTS formation.

The crystallinity of the absorbers were analyzed by X-ray diffraction (XRD) using an X'Pert PRO (PANalytical B.V., Holland) diffractometer with high-intensity Cu Kα1 irradiation (λ=1.5406 Å). The surface and cross-section morphologies of the films were characterized using scanning electron microscopy (SEM, A Nova NanoSEM 450) operated at 5 kV. The chemical compositions of the films were measured by X-ray fluorescence (XRF, UX-220 of Huawei).

To complete the solar cell devices, a CdS buffer layer of 60 nm thickness was firstly deposited on the CZTS thin film by chemical bath deposition (CBD). A 300 nm thick i-ZnO/ZnO:Al layer was then prepared as transparent conducting layer by rf-sputtering. Finally, Ni/Al metal grids were deposited by e-beam evaporation through an aperture mask to form current collector. The solar cell device was scribed into cells with area of ~0.5 cm^2 each and the J-V performance was measured under a simulated AM 1.5 Global spectrum. The illumination intensity of 100 mW/cm^2 was calibrated using a certified silicon solar cell.

3. Results and Discussions

3.1 Sulfuration temperature effect

To study the sulfuration temperature effect on the Sn loss for the co-sputtered precursors, the annealing processes were carried out at different peak temperature of 440℃, 470℃, 500℃ and 520℃, respectively, in the N_2+H_2S atmosphere with a H_2S concentration of 5%. The sample temperatures were ramped from room temperature to the set values at a rate of 5℃/min and maintained at the peak temperatures for 15 minutes before they were cooled down naturally. The compositions in all the precursors were designed to be about Cu/Sn= 1.31 and Cu/Zn=1.54.

Figure 1(a) showed the XRD spectra of CZTS films prepared at different sulfuration temperatures, revealing a polycrystalline kesterite CZTS crystal structure with major reflections along the (112), (200), (220) and (312) planes (JCPDS ＃00-026-0575). To exclude the possible existence of the Cu_2SnS_3 phase with similar XRD peaks, Raman measurement was performed. Raman spectra only gave characteristic CZTS peaks[15] at 287 cm^{-1}, 338 cm^{-1} and 368 cm^{-1}. With increasing sulfuration temperature, the (112) XRD peak became more intense and sharper, which indicated that the crystalline quality of the CZTS thin films was improved. In addition to the four

XRD peaks originated from CZTS, one additional peak around 31.9° was always found for samples sulfurized at low temperatures, e.g., 440℃ and 470℃. This peak matched the characteristic peak of SnS (JCPDS No. 14-0620) very well. Its intensity dropped quickly when the sulfuration temperature was increased above 440℃ and could not be observed at temperatures higher than 500℃. In our experiment, we used SnS_2 as the source for Sn and the observed SnS in the samples must come from the decomposition of SnS_2 in the precursor during thermal treatment. It is well noticed that SnS has a high vapor pressure and can be vaporized at high temperature. The absence of SnS and Cu_2SnS_3 related secondary phases in the thin films prepared at temperatures above 500℃ suggested that the peak sulfuration temperature was very important in eliminating Sn-related secondary phases. Manipulating Sn-loss process by peak temperature could produce a pure CZTS film.

To more clearly demonstrate the sulfuration temperature effect on the Sn loss, we plotted the ratio of Cu/Sn in the samples against sulfuration temperature, as shown in Figure 1(b). Since copper sulfides would not evaporate under these conditions, the change of Cu/Sn actually reflected the loss of Sn content. It could be seen that Cu/Sn at 440℃ was almost the same as that in the precursor. This ratio increased to 1.43 at 470℃ by losing 10% of Sn in the precursors, indicating the start of SnS evaporation, which was in good agreement with the decrease of SnS peak observed in the XRD spectra. When the sulfuration temperature was at 500℃, all the excess Sn in the form of SnS secondary phase was gone and the ratio of Cu/Sn approached to 1.7-1.8. This value was close to the favored ratio in high efficiency devices with Cu/(Zn+Sn) ~ 0.8 and Zn/Sn ~1.1-1.2. When the temperature was further increased to 520℃, the evaporation of Sn continued and Cu/Sn moved to 1.9 - 2.0. The loss of Sn in our samples at sulfuration temperature around 520℃ was believed to originate from the decomposition of CZTS as similarly reported before[10]. The instability of CZTS compound during annealing at temperatures higher than 520℃ was relevant to the instability of Sn^{4+} against reduction[11] in the absence of sufficient and large sulfur pressure. If the sulfuration temperature was even higher than 520℃, Cu/Sn would be larger than 2, seeing a Cu-poor to Cu-rich transition in the CZTS thin film.

The upper and lower panels of Figure 2 displayed the plane and cross-section SEM images of CZTS films sulfurated at various substrate temperatures. As shown in 2(a) and 2(e), the crystallization of CZTS could already be clearly observed in the thin film after being treated at 440℃, though the grain size was still small. For a ~1.0 μm thick film, it usually consisted of 3 to 4 layers of grains across the depth direction. At higher treatment temperatures such as 500℃, as shown in Figure 2(c) and 2(g), the grains became much larger with a size over 500 nm. The morphology of the thin film treated at 520℃ was similar to that at 500℃. For samples sulfurized at higher temperatures, it was found that more voids near the interface between the CZTS thin film and Mo substrate would be present, as shown in Figure 2(d) and 2(h), possibly originating from the strong vaporization of SnS at high temperatures. As the sulfuration temperature increased, the surface roughness of the thin film showed an obvious increase as the crystal size became larger, which might present challenges for the thin CdS buffer layer preparation to achieve perfect coverage of the surface in the latter stage of device fabrication.

The performance parameters of the devices with CZTS thin films sulfurized at different

temperatures were listed in Table I. For device made of thin film sulfurized at 440°C, small short-circuit current density (J_{SC}) and poor fill factor (FF) were observed to be the reason for the poor conversion efficiency, which may partly originated from the existence of SnS secondary phase. At higher sulfuration temperature of 520°C, degradation of device performance was also found, which was attributed to the deviation of the absorber composition away from the favored copper-poor and Sn-rich phase due to the further loss of Sn content by decomposition of CZTS. In this experiment, we identified that a sulfuration temperature in the range of 500-520°C was suitable to fabricate CZTS thin films free of secondary phase like SnS without showing remarkable decomposition. Here, we had to clarify that the above mentioned optimized temperature was actually dependent on the composition of the precursors and the sulfuration atmosphere such as H_2S content, which would be discussed in the latter parts of this paper.

3.2 H_2S concentration effect

To investigate the effect of H_2S concentration in the sulfuration atmosphere of N_2+H_2S on the Sn composition and other properties of the CZTS thin films, we employed various H_2S concentration of 2.5%, 5% and 7.5% during the thermal processing. We took the optimized sulfuration conditions from Section 3.1, namely, first ramping the substrate temperature at a rate of 5℃/min from room temperature to the optimal peak temperature of 500℃ and then maintaining the substrate at the peak temperature for 15 minutes. Again, the precursor was made to be Sn-rich with composition of Cu/Sn= 1.05 and Cu/Zn=1.54.

Figure 3 showed the Cu/Sn in the CZTS thin films prepared with different H_2S concentrations. For samples sulfurized with a H_2S concentration higher than 5%, the ratio of Cu/Sn changed from 1.05 in the precursor to around 1.5 in the film, which indicated that 30% of the Sn atoms were lost. For the sample sulfurized with a H_2S concentration of 2.5%, Cu/Sn was about 1.3, suggesting that only 16% of the Sn atoms were lost. Since decomposition of CZTS at 500°C was not obvious, the loss of Sn in the experiment was believed to come from the evaporation of SnS. The observed smaller Sn loss rate at lower H_2S concentration was believed to come from two reasons. The first reason was that there was a phase separation due to the diffusion limited sulfur incorporation in the crystallization process. When H_2S was insufficient, the prepared sample was always seen to have big and compact crystallites near the surface but tiny ones at the bottom of the layer (as shown in Figure S1). Microscopic energy dispersive spectroscopy (EDS) revealed that the bottom layer is with much higher Sn composition (as shown in Figure S1(d)). Raman spectrum measured at the bottom surface (after peeling off the film from the Mo substrate) also displayed SnS related weak peaks at 163 cm^{-1}, 191 and 218 cm^{-1}. The excess SnS in the Sn-rich precursors was mostly left underneath the CZTS crystals after thermal treatment in the atmosphere with low H_2S concentration, which made the SnS evaporation process to be much slower because of the compact CZTS film on the top. This phase separated growth under sulfur-poor condition could be well explained by the crystallization process limited by the sulfur diffusion since S had to diffuse across the surface layer before it can react with the precursors underneath. The second reason might come from the reaction between SnS and H_2S which resulted in a faster Sn loss at higher H_2S concentration. Though the evaporation of solid SnS was commonly thought to mainly occur by forming SnS vapor, the research by Shimada et al.[16]

showed that Sn element could actually volatilize as gasous SnS_3 through the following way:

$$SnS(s) + 2S \rightarrow SnS_3(g)$$

This reaction implied that higher partial pressure of S would facilitate the formation of SnS_3 and accelerate the loss of Sn, partly explaining the faster loss of SnS with higher H_2S concentrations as observed in our experiment. To eliminate the possible SnS secondary phase, in our experiment, we found that the concentration of H_2S in the sulfuration atmosphere should be high enough. However, too much H_2S should also be avoided since it would lead CZTS to peel off from the Mo electrodes due to the heavy sulfuration of Mo.

Table II presented the performance parameters for devices fabricated with CZTS annealed using different H_2S concentrations. For the 2.5% case, device had poor efficiency since large amount of SnS phase were found to be left in the material. For H_2S concentration higher than 5%, devices showed much higher efficiency due to the increased open circuit voltage (V_{oc}) and short circuit current density (J_{sc}) .

3.3 Temperature ramping rate effect

The temperature ramping rate effect on the properties of CZTS thin films had been studied by several groups[8, 17-19]. Large crystals could be prepared both at a slow ramping rate of 2°C/min and a fast rate of 100°C/min. The difference between the fast and slow ramping rate was helpful in identifying the reaction pathways to form the quaternary phase. Different from our case here, the previous studies were mainly for precursors made of elemental metals. Moreover, variations of the precursor composition might also have important influence on the formation reactions dynamics. Here, we studied the ramping rate effect on the Sn-loss using co-sputtered $ZnS/SnS_2/Cu$ precursors. The composition in the precursor was about Cu/Sn= 1.05 and Cu/Zn=1.54. The sulfuration temperature was set at 500℃ for 15 minutes and the H_2S concentration was 5%.

Remarkable morphological differences were observed among samples treated with different temperature ramping rate. Cross-sectional SEM pictures (as shown in Figure S2) showed that CZTS thin films were compact with large grains for ramping rate at 3, 5 and 12°C/min, while samples annealed with ramping rate at 12°C/min or above evidenced the presence of exploded bubbles which resulted in plenty of crystallites lost their contacts with the Mo substrate.

Figure 4 showed the ratio of Cu/Sn in the CZTS thin films prepared with different ramping rate. Generally, it showed an increasing Sn loss with increasing ramping rate. A rapid ramping process at 12°C/min showed a very high Cu/Sn ratio of 5.5 and suggested that 80% of Sn had evaporated during the thermal process, leading the thin film to be Cu-rich. We believed that the loss of Sn was due to the vaporization of SnS at high ramping rate under which SnS in the precursor was not effectively absorbed by other binaries to form stable ternary or quaternary crystallites before it experienced high speed evaporation at high temperatures.

Table III presented the performance parameters of devices prepared with different ramping rate. Samples treated with 3°C/min and 5°C /min ramping rate had conversion efficiencies above

4%, while the sample treated with 12°C /min ramping rate showed very poor properties.

It was concluded that, in our case for the co-sputtered sulfur containing binary precursors, a slow ramping (5°C/min or smaller) was superior to a rapid one. A smaller ramping rate helped the incorporation of Sn atoms into the alloy by avoiding the vaporization of SnS before it reacted with Cu_2S and ZnS. The morphological differences also revealed the advantages of the slow ramping rate to obtain CZTS absorbers with compact crystallites and large grains.

3.4 Zn content effect

In addition to the above mentioned parameters, we found that the Sn loss in CZTS thin films was also strongly dependent on the Zn content in the precursor, which has been overlooked in previous studies. To study the Zn content effect, we prepared precursors with Cu/Zn varied from 1.1 to 1.6 while keeping Cu/Sn to be 1.25. The samples were sulfurized at 510℃ and 530℃ respectively for 15 minutes, with a ramping rate of 5℃/min and a H_2S concentration of 5%.

Figure 5 showed the ratio of Cu/Sn in the CZTS thin films after thermal treatment. With peak temperature at 530℃, the samples with different Zn contents were always found to have Cu/Sn in the range of 2-2.1, indicating that the thin films were in a Sn-poor phase. The Sn loss was believed to originate from the decomposition of CZTS at this temperature, as discussed in Section 3.1. There had several publications which employed sulfuration temperatures higher than 530℃[1, 2, 5, 20] without showing serious CZTS decomposition with high S pressure, possibly due to the increased stability of Sn^{4+} against reduction with sufficient sulfur vapor. For the samples sulfurized at 510℃, Cu/Sn showed an decreasing trend with the increase of Zn content in the precursors. Since CZTS at temperatures of 510℃ or lower did not suffer noticeable decomposition under our experiment conditions, the loss of Sn mainly came from the vaporization of volatile SnS phase which was decomposed from SnS_2 in the precursors during the temperature ramping stage. We believed that the increased ZnS density in a Sn-rich precursor would certainly accelerate the following reaction,

$$Cu_2S + ZnS + SnS_2 \rightarrow Cu_2ZnSnS_4 .$$

A high ZnS reactant would accelerate the crystallization process by effectively turning the unstable SnS_2 into CZTS by the free energy consideration, which could well explain the reduced Sn loss in samples with higher Zn content in the precursors.

Table IV showed the performance parameters of devices with different Zn contents in the precursors. It was generally found that higher Zn content in the precursor would be very helpful in achieving higher Voc in the devices. The device with the highest Voc was sample D which showed conversion efficiency around 6.39%. Even without anti-reflection layer in our device, this conversion efficiency was already comparable to that of the record efficiency of 6.7% made by Katagiri's group using sputtered precursors.

Based on the above understanding of the sulfuration conditions, we recently designed a novel two-step sulfuration/annealing process using the conditions of sample D as the baseline. The two-stage process, which will be described in details elsewhere, is to firstly treat the precursor at low temperature for a longer time and then anneal the thin film at high temperature for a shorter

time to improve the crystalline quality. The CZTS phase was to form at the low temperature stage without any worry for the loss of Sn, while pure phase large grains were obtained at high temperature stage by merging small crystals and evaporating excess SnS phase. The key here is the employment of SnS_2 as the precursor, so that homogeneous CZTS thin film can readily form at the low-temperature stage. When SnS or Sn was used as precursor, CZTS thin films were easily found to be with layered and phase separated structure due to the insufficient sulfur incorporation in the precursor. The temperature for the first stage was usually set to be slightly lower than 280℃ where SnS_2 was not seriously decomposed into volatile SnS. The overall composition of the CZTS thin film fabricated using a two-stage process was found to be similar to that of sample D (6.39%), while the vertical distribution of all the elements in the former were much more homogeneous, especially for Zn. The best device fabricated using the two-stage process was listed here as device F* which had a conversion efficiency of 8.5%. To our knowledge, the highest ever reported conversion efficiency of CZTS devices was 8.4% using a co-evaporation-sulfuration approach. Our result showed that sputtering-sulfuration approach could also produce devices with performance comparable or even better than that of co-evaporation. A note to add is that device F* was capped by an anti-reflection (AR) coating of MgF_2 layer, while all other devices were not coated with AR layers.

From the above experimental results, we could find that the remaining Sn contents in the CZTS thin films would undoubtedly be affected by the Zn composition in the precursors. Samples with excess ZnS in the precursors showed less Sn loss, which made the absorbers more Cu-poor in the sense of the ratio of Cu/(Zn+Sn). One clear observation was that the increased Zn composition in the precursor significantly improved the Voc in the devices. Using admittance spectroscopy, we identified that the density of hole traps with activation energy around 100 meV was effectively suppressed due to the Zn-rich condition, when Cu/Zn decreased from 1.57 to 1.15. We attributed this to the reduced density of ionized Cu_{Zn} defects[21] under Zn-rich growth condition. The ionized Cu_{Zn} defects were shown to cause potential fluctuations[22] of the valence band due to the Coulomb attraction, which would induce the trapping of the photo-generated holes in the local potential minimums and therefore lower the Voc in devices.

4. Conclusions

We have systematically examined various sulfuration conditions in order to optimize the performance of CZTS absorbers. Starting from highly Sn-enriched precursors prepared by co-sputtering Cu, ZnS and SnS_2 targets, the Cu/Sn ratio in the prepared thin films have been studied by varying post-sulfuration parameters such as the peak annealing temperature, H_2S concentration in the atmosphere, temperature ramping rate, and Zn contents in the precursors. Peak annealing temperature above 500℃ was found helpful in eliminating SnS related secondary phase, but temperatures higher than 530℃ would produce Sn-poor CZTS with Cu/Sn > 2 due to the Sn loss originated from the decomposition of CZTS. A slow temperature ramping rate and sufficient H_2S concentration were found necessary for complete reaction of the precursors. Excess ZnS in the precursor were also found to reduce the Sn loss and evidently improve Voc in the devices. To make the CZTS composition fall in the desired region, the sulfuration/annealing parameters discussed above must be carefully designed and controlled to match the initial

compositions of the precursors.

Acknowledgments: This work is supported by 973 project of China under 2012CB933700, NSF of China under 61274093 and 51302304, 51302303. We will also thank ITC funding of Shen Zhen under projects KQC201109050091A and JCYJ20120617151835515.

References:

1. W. Wang, M. T. Winkler, O. Gunawan, T. Gokmen, T. K. Todorov, Y. Zhu and D. B. Mitzi, *Adv. Energy Mater.*, 2013, 4, 1301465.
2. B. Shin, O. Gunawan, Y. Zhu, N. A. Bojarczuk, S. J. Chey and S. Guha, *Progress in Photovoltaics: Research and Applications*, 2013, 21, 72-76.
3. I. Repins, C. Beall, N. Vora, C. DeHart, D. Kuciauskas, P. Dippo, B. To, J. Mann, W.-C. Hsu, A. Goodrich and R. Noufi, *Sol. Energy Mater. Sol. Cells*, 2012, 101, 154-159.
4. I. D. Olekseyuk, I. V. Dudchak and L. V. Piskach, *J. Alloys Compd.*, 2004, 368, 135-143.
5. H. Katagiri, K. Jimbo, S. Yamada, T. Kamimura, W. S. Maw, T. Fukano, T. Ito and T. Motohiro, *App. Phys. Exp.*, 2008, 1, 041201.
6. K. Wang, O. Gunawan, T. Todorov, B. Shin, S. J. Chey, N. A. Bojarczuk, D. Mitzi and S. Guha, *Appl. Phys. Lett.*, 2010, 97, 143508.
7. L. Grenet, S. Bernardi, D. Kohen, C. Lepoittevin, S. Noël, N. Karst, A. Brioude, S. Perraud and H. Mariette, *Sol. Energy Mater. Sol. Cells*, 2012, 101, 11-14.
8. R. B. V. Chalapathy, G. S. Jung and B. T. Ahn, *Sol. Energy Mater. Sol. Cells*, 2011, 95, 3216-3221.
9. C. Platzer-Björkman, J. Scragg, H. Flammersberger, T. Kubart and M. Edoff, *Sol. Energy Mater. Sol. Cells*, 2012, 98, 110-117.
10. A. Weber, R. Mainz and H. W. Schock, *J. Appl. Phys.*, 2010, 107, 013516.
11. J. J. Scragg, T. Ericson, T. Kubart, M. Edoff and C. Platzer-Björkman, *Chem. Mater.*, 2011, 23, 4625-4633.
12. A. Redinger, D. M. Berg, P. J. Dale and S. Siebentritt, *J. Am. Chem. Soc.*, 2011, 133, 3320-3323.
13. A. Redinger and S. Siebentritt, *Appl. Phys. Lett.*, 2010, 97, 092111.
14. H. Katagiri, K. Jimbo, W. S. Maw, K. Oishi, M. Yamazaki, H. Araki and A. Takeuchi, *Thin Solid Films*, 2009, 517, 2455-2460.
15. X. Fontane, L. Calvo-Barrio, V. Izquierdo-Roca, E. Saucedo, A. Perez-Rodriguez, J. R. Morante, D. M. Berg, P. J. Dale and S. Siebentritt, *Appl. Phys. Lett.*, 2011, 98, 181905.
16. T. Shimada, F. S. Ohuchi and B. A. Parkinson, *J. Vac. Sci. Technol., A*, 1992, 10, 539-542.
17. A. Ennaoui, M. Lux-Steiner, A. Weber, D. Abou-Ras, I. Kötschau, H. W. Schock, R. Schurr, A. Hölzing, S. Jost, R. Hock, T. Voß, J. Schulze and A. Kirbs, *Thin Solid Films*, 2009, 517, 2511-2514.
18. K. Maeda, K. Tanaka, Y. Fukui and H. Uchiki, *Sol. Energy Mater. Sol. Cells*, 2011, 95, 2855-2860.
19. J. Ge, Y. Wu, C. Zhang, S. Zuo, J. Jiang, J. Ma, P. Yang and J. Chu, *Appl. Surf. Sci.*, 2012, 258, 7250-7254.
20. H. Xin, J. K. Katahara, I. L. Braly and H. W. Hillhouse, *Adv. Energy Mater.*, 2014, 4, 1301823.
21. S. Chen, A. Walsh, X.-G. Gong and S.-H. Wei, *Adv. Mater.*, 2013, 25, 1522-1539.

22. M. J. Romero, H. Du, G. Teeter, Y. Yan and M. M. Al-Jassim, *Phys. Rev. B: Condens. Matter*, 2011, 84, 165324.

Figure captions

Figure 1. (a) XRD spectra, (b) Cu/Sn and remaining Sn content in CZTS films annealed at different temperatures

Figure 2. Plane (upper pannel) and Cross-section (lower pannel) SEM pictures of CZTS films annealed at different temperatures. (a) and (e) are at 440℃. (b) and (f) are at 470℃. (c) and (g) are at 500℃. (d) and (h) are at 520℃.

Figure 3. Cu/Sn and remaining Sn in the thin films annealed at different H_2S concentrations of 2.5%, 5% and 7.5%, respectively.

Figure 4. Cu/Sn and remaining Sn content in thin films with different heating rates of 3℃/min, 5℃/min and 12℃/min, respectively.

Figure 5. Cu/Sn in the devices with different Zn content.

Tables

Table I. Performance parameters of devices annealed at different annealing peak temperatures

Table II. Performance parameters of devices annealed at different H_2S concentrations

Table III. Performance parameters of devices annealed with different temperature ramping rates

Table IV. Performance parameters of devices with different Cu/Zn in the precursors

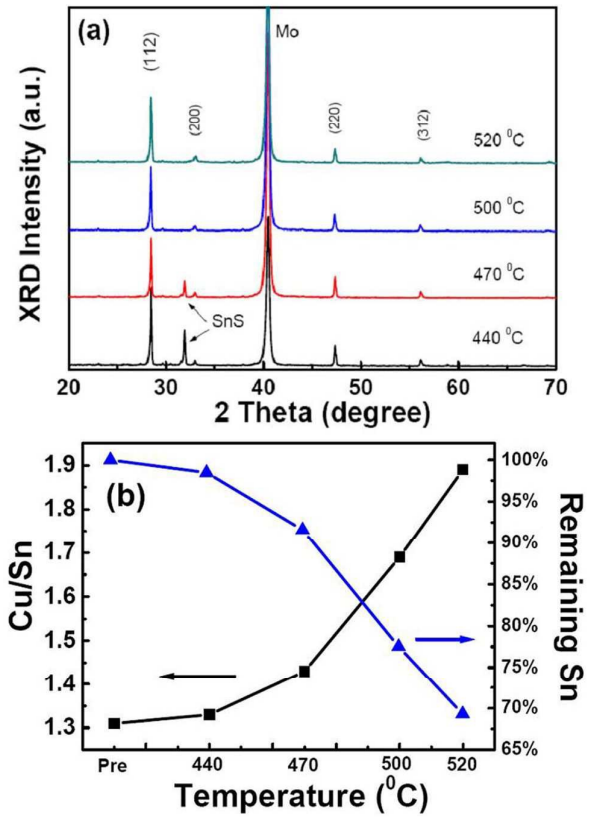

Figure 1. (a) XRD spectra, (b) Cu/Sn and remaining Sn content in CZTS films annealed at different temperatures

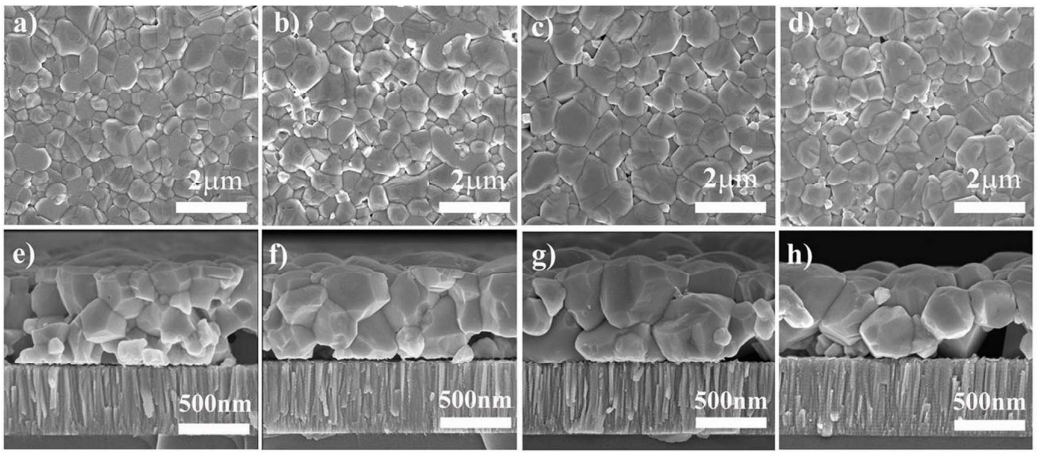

Figure 2. Plane (upper pannel) and Cross-section (lower pannel) SEM pictures of CZTS films annealed at different temperatures. (a) and (e) are at 440℃. (b) and (f) are at 470℃. (c) and (g) are at 500℃. (d) and (h) are at 520℃.

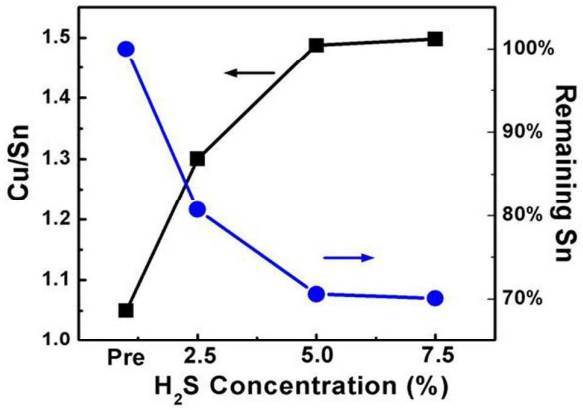

Figure 3. Cu/Sn and remaining Sn in the thin films annealed at different H_2S concentrations of 2.5%, 5% and 7.5%, respectively.

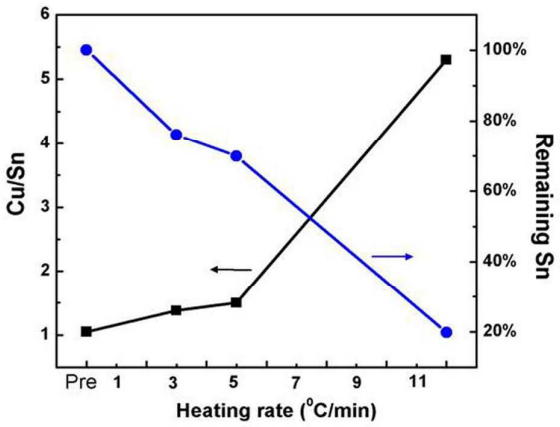

Figure 4. Cu/Sn and remaining Sn content in thin films with different heating rates of 3℃/min, 5℃/min and 12℃/min, respectively.

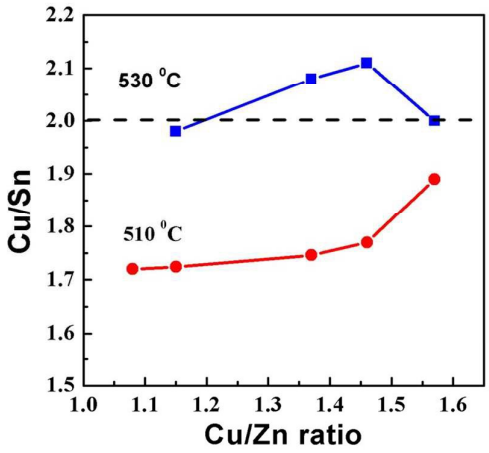

Figure 5. Cu/Sn in the devices with different Zn contents.

Tables

Table I. Performance parameters of devices annealed at different annealing peak temperatures

Temp(℃)	Voc(mV)	Jsc(mA/cm^2)	FF	Efficiency
440℃	533	10.2	0.38	2.03%
470℃	526	14.4	0.52	3.93%
500℃	535	14.4	0.55	4.18%
520℃	559	12.6	0.53	3.71%

Table II. Performance parameters of devices annealed at different H_2S concentrations

Rate	Voc(mV)	Jsc(mA/cm^2)	FF	Efficiency
2.5%	298	8.09	0.46	1.11%
5.0%	574	14.04	0.51	4.11%
7.5%	597	14.68	0.46	4.03%

Table III. Performance parameters of devices annealed with different temperature ramping rates

Rate	Voc(mV)	Jsc(mA/cm^2)	FF	Efficiency
3℃/m	569	15.7	0.55	4.91%
5℃/m	597	14.7	0.46	4.04%
12℃/m	301	2.13	0.51	0.33%

Table IV. Performance of devices with different Cu/Zn in the precursors

Sample	Cu/Zn	Voc(mV)	Jsc(mA/cm^2)	FF	Efficiency
A	1.57	537	14.2	0.58	4.47%
B	1.46	553	13.6	0.56	4.22%
C	1.37	561	15.2	0.58	4.88%
D	1.15	640	17.4	0.58	6.39%
E	1.08	580	14.4	0.59	4.92%
F*	1.24	625	21.8	0.63	8.57% (AR)

Table of contents entry

The elements contents and the annealing parameters, such as the peak annealing temperature, H2S concentration and ramping rate would strongly affect the remaining Sn contents in the Cu_2ZnSnS_4 thin films and greatly influence the device performance.